

## Tropical cyclone inundation potential on the Hawaiian Islands of Oahu and Kauai

Andrew B. Kennedy<sup>a,\*</sup>, Joannes J. Westerink<sup>a</sup>, Jane M. Smith<sup>b</sup>, Mark E. Hope<sup>a</sup>, Michael Hartman<sup>a</sup>, Alexandros A. Taflanidis<sup>a</sup>, Seizo Tanaka<sup>a,e</sup>, Hans Westerink<sup>a</sup>, Kwok Fai Cheung<sup>c</sup>, Tom Smith<sup>d</sup>, Madeleine Hamann<sup>a</sup>, Masashi Minamide<sup>e</sup>, Aina Ota<sup>e</sup>, Clint Dawson<sup>f</sup>

<sup>a</sup> Department of Civil Engineering and Geological Sciences, University of Notre Dame, Notre Dame, IN 46556, USA

<sup>b</sup> Coastal and Hydraulics Laboratory, US Army Engineer Research and Development Center, 3909 Halls Ferry Road, Vicksburg, MS 39180, USA

<sup>c</sup> Department of Ocean and Resources Engineering, University of Hawaii at Manoa, 2540 Dole Street, Holmes Hall 402, Honolulu, HI 96822, USA

<sup>d</sup> US Army Corps of Engineers, Honolulu District, Bldg. 230, CEPOH-EC-R, Fort Shafter, HI 96858-5440, USA

<sup>e</sup> Department of Civil Engineering, University of Tokyo, Faculty of Engineering Bldg. 1/11, Hongo Campus, 7-3-1 Hongo Bukkyo-ku, Tokyo 113-8656, Japan

<sup>f</sup> Department of Aerospace Engineering and Engineering Mechanics, The University of Texas at Austin, 210 East 24th Street, W.R. Woolrich Laboratories, 1 University Station, C0600 Austin, TX 78712-0235, USA

### ARTICLE INFO

#### Article history:

Received 13 December 2011

Received in revised form 25 April 2012

Accepted 30 April 2012

Available online 29 May 2012

#### Keywords:

Hurricanes  
Water waves  
Wave runup  
Storm surge  
Storm inundation  
Hurricane Iniki  
Hawaii

### ABSTRACT

The lack of a continental shelf in steep volcanic islands leads to significant changes in tropical cyclone inundation potential, with wave setup and runup increasing in importance and wind driven surge decreasing when compared to more gently-sloped mainland regions. This is illustrated through high resolution modeling of waves, surge, and runup on the Hawaiian Islands of Oahu and Kauai. A series of hurricane waves and water levels were computed using the SWAN + ADCIRC models for a suite of 643 synthetic storm scenarios, while local wave runup was evaluated along a series of 1D transects using the phase-resolving model Bouss1D. Waves are found to be an extremely important component of the inundation, both from breaking wave forced increases in storm surge and also from wave runup over the relatively steep topography. This is clear in comparisons with debris lines left by Hurricane Iniki on the Island of Kauai, where runup penetration is much greater than still water inundation in most instances. The difference between steeply-sloping and gently-sloping topographies was demonstrated by recomputing Iniki with the same landfall location as Hurricane Katrina in Louisiana. Surge was greatly increased for the mild-slope Iniki-in-Louisiana case, while pure wind surge for Iniki-in-Kauai was very small.

For the entire suite of storms, maxima on Kauai show predicted inundation largely confined to a narrow coastal strip, with few locations showing more than a few hundred meters of flooding from the shoreline. As expected, maximum flooded areas for the 643 storms were somewhat greater than the Iniki inundation.

Oahu has significantly more low-lying land compared to Kauai, and consequently hypothetical tropical cyclone landfalls show much more widespread inundation. Under direct impact scenarios, there is the potential for much of Honolulu and most of Waikiki to be inundated, with both still water surge and wave runup contributing. Other regions of Oahu show inundation confined to a more narrow coastal strip, although there is still much infrastructure at risk.

Even for very strong storms in Oahu and Kauai, maximum still water surge is relatively small, and does not exceed 3 m in any storm modeled. In contrast, hurricane waves several kilometers from shore regularly exceed 10 m due to the lack of a continental shelf.

© 2012 Elsevier Ltd. All rights reserved.

### 1. Introduction

Landfalling tropical cyclones are a major source of damaging winds, waves and surge, causing hundreds of billions of dollars in damage to the United States over the past decade (Blake and

Landsea, 2011). In the continental United States, hurricanes tend to make landfall in regions with a relatively broad, gently sloping continental shelf that is tens to hundreds of kilometers wide (Hurricane Katrina, 2005; Hurricane Ike, 2008; Hurricane Irene, 2011, [nhc.noaa.gov](http://nhc.noaa.gov)). However, oceanic volcanic islands do not have continental shelves and water depths of hundreds to thousands of meters may be within a few kilometers of shore. For this reason, the important processes in inundation also change. For

\* Corresponding author. Tel.: +1 574 631 6686; fax: +1 574 631 9236.

E-mail address: [andrew.kennedy@nd.edu](mailto:andrew.kennedy@nd.edu) (A.B. Kennedy).

steady-state conditions, this may be shown by the one-dimensional steady-state storm surge balance (e.g. Dean and Darymple, 1991)

$$g \frac{\partial \eta}{\partial x} = \frac{\tau_s}{\rho(h + \eta)} - \frac{1}{\rho(h + \eta)} \frac{\partial S_{xx}}{\partial x} - \frac{1}{\rho} \frac{\partial P_a}{\partial x} \quad (1)$$

where  $\eta$  and  $h$  are the water surface elevation and depth, respectively,  $g$  is gravitational acceleration,  $\rho$  is the water density,  $\tau_s$  is the wind surface stress,  $S_{xx}$  is the wave radiation stress, and  $P_a$  is the atmospheric pressure. Other terms will appear for two-dimensional, unsteady cases and when considering three-dimensional motions, but the basic cross-shore force balance is largely the same. For a wide continental shelf, surge is dominated by the integration of surface wind stresses over a long distance, with atmospheric pressure variations, wave setup, and wave modification to surface drag (e.g. Mastenbroek et al., 1993) also playing roles. However, as continental shelves shrink but the storm size remains constant, the contribution from wind stresses integrated over the shelf becomes much smaller because the integration distance is much shorter. In contrast, the pressure term remains the same, as it has no depth dependence. The wave setup contribution will increase in magnitude, as its value at the shoreline is proportional to the breaking wave height (Dean and Darymple, 1991), which can be very large in regions with deep water close to shore. Waves may partially reflect from steep-fronted reefs, while wind-wave reflection is negligible on gentle continental shelves. Thus, surge and inundation response is expected to be much different from that in mainland regions.

A further difference lies at the immediate shoreline. In very flat regions subject to surge, waves may be relatively small at the shoreline and thus wave runup is not very important. However, in regions like the Hawaiian Islands where large waves can propagate close to shore and shorelines may be relatively steep, wave runup can greatly increase storm inundation over still water surge (e.g., Cheung et al., 2003). Thus it becomes essential to include wave runup in all estimates of storm inundation for steep volcanic islands.

The Hawaiian Islands are classic examples of islands with no continental shelf. While they typically experience very mild weather, historical hurricanes have produced severe consequences. By far the most devastating storm in recent years was in 1992, when Hurricane Iniki made a direct landfall on the island of Kauai as a Category 4 storm on the Saffir-Simpson scale, with a central pressure of 945 millibars (mbar) and 140 mph (63 m/s) winds. Impacts were severe, with \$1.8 billion damage, over 1400 homes completely destroyed and 10 times that number damaged in a relatively sparsely populated island (US Department of Commerce, 1993; Post et al., 1993). If a storm like Iniki had instead made landfall in Honolulu, impacts would have been even greater. Kauai was further impacted by Hurricane Iwa in 1982, which passed by as a strong category 1 storm. Other notable storms include Hurricane Dot (1959), which passed just off the coast of Hawaii, Oahu, and Kauai; Hurricane Nina (1957), which passed offshore of Kauai; and the Kohala cyclone of 1871, which caused great damage on the islands of Hawaii and Maui (Central Pacific Hurricane Center, <http://www.prh.noaa.gov/hnl/cphc/>); other hurricanes are known from the historical record. This infrequency combined with the large potential severity means that hurricanes in the Hawaiian Islands behave more like tsunamis in return frequency than typical hurricane-prone regions. Because of this, true return periods are difficult to obtain. Thus, it is useful to examine the inundation caused by different hurricane scenarios to determine potential areas of danger in the event of an oncoming landfall, and for determining evacuation routes, emergency shelter locations, and other longer term planning.

## 2. Inundation modeling on Oahu and Kauai

As part of the United States Army Corps of Engineers Surge and Wave Island Modeling Studies (SWIMS), inundation was computed for a suite of 643 possible hurricanes in the vicinity of Oahu and Kauai. Two sets of models were used: the first suite was the SWAN + ADCIRC wave and circulation models (Zijlema, 2010; Dietrich et al., 2011), and the second was a 1D phase-resolving Boussinesq surf zone model used to compute wave group inundation (Demirbilek et al., 2009).

### 2.1. SWAN + ADCIRC modeling

The SWAN + ADCIRC modeling system can compute combined wave-current-water level evolution over scales ranging from 10 s of meters to thousands of kilometers using coupled spectral wave and shallow water models. The system was run on an unstructured grid from 0 to 30°N, and 139 to 169°W and forced by hurricane wind and pressure fields. Bathymetry and topography were generated using many different datasets: bathymetric and topographic lidar in shallow water and on dry land, shipboard multibeam bathymetry from ocean cruises in deeper coastal regions, and NOAA bathymetric databases. The resulting 3.5 million element unstructured triangular grid was used to compute wave heights and surge levels with resolutions ranging from 30 m in shallow water and overland to 10 km in the deep ocean. Wind drag was computed using a Garratt formulation and bottom drag was computed with a Manning's  $n$  formulation. The USGS GAP land cover database was used to specify the bottom friction coefficient according to the vegetation cover or land use type as specified in Bunya et al. (2010). Nearshore reefs were identified by hand where possible and given a large frictional value of  $n = 0.22$ , and oceanic areas with no other classification were specified to have  $n = 0.02$ . The wave model SWAN used 72 directional bins and 45 frequency bins to compute spectral wave characteristics. Wave physics used standard third generation formulation with Cavaleri and Malanotte-Rizzoli (1981) wave growth and shallow water triad terms activated. Both SWAN and ADCIRC were run on the same grid. The ADCIRC time step was 1 s, the SWAN time step was 600 s, and two-way coupling was performed after each SWAN time step as described in Dietrich et al. (2011). Full spectral radiation stresses were computed by SWAN, integrated and output to ADCIRC, and provided additional nearshore forcing for wave setup and currents. These are the same tools used for studies of storm surge on the US mainland (e.g. Bunya et al., 2010; Dietrich et al., 2010), and the models provide high fidelity estimates of wave heights and water levels (surge) in regions covered by water during a storm.

Because SWAN and ADCIRC are large-scale models, waves are phase-averaged and thus individual wave crests and troughs do not appear in the model. Instead, phase-averaged properties from the wave model (SWAN) are fed into the circulation model (ADCIRC) through radiation stresses, which force significant setup (increase in water level) and strong currents in regions of wave breaking near the shore. These SWAN + ADCIRC inundation estimates are defined as *still water inundation*, or *surge*, and denote an average water level over periods of around 10 min. The downside of these models is that individual wave crests and slowly varying wave groups generate infragravity waves that can penetrate significantly further inland than is predicted by the phase-and-spectrally-averaged models (e.g., Mase, 1989). This *wave runup* inundation is particularly significant in regions without a continental shelf such as the Hawaiian Islands, where large waves propagate close to shore, and inland penetration can cause significant damage as was seen during Hurricane Iniki.

## 2.2. Phase-resolving Boussinesq modeling

To model wave runup requires a second tool, and a Boussinesq model was used to compute shoreline runup in excess of the wave-averaged surge. Boussinesq-type models represent each wave at many points along its length, with individual crests and troughs modeled in high resolution (Nwogu, 1993). Because of this, they are very good at representing wave group effects and partial reflection from complex topographies. With the addition of wave breaking and a time-varying shoreline, they can also model runup quite well (Kennedy et al., 2000; Nwogu and Demirbilek, 2010). The downside of Boussinesq and other phase-resolving models is that they are much more computationally expensive than phase-averaged models such as SWAN.

This is particularly true for two-dimensional Boussinesq models which would require approximately 5 m resolution around the entire coastlines of Oahu and Kauai to several kilometers offshore, and as far inland as the extent of inundation. For domains of this size, computational technology has not yet advanced to the point where full two-dimensional Boussinesq models may be run for hundreds of scenarios. Thus, the one-dimensional phase-resolving model Bouss1D (Demirbilek et al., 2009) was run along one-dimensional cross-shore transects with 5 m resolution on both islands. The model was initialized at 40 m water depth, which in many cases was quite close to the shore. If the 40 m depth contour was not reached by 2 km offshore, the depth at 2 km was used instead. Waves and surge at the transect origin were output from the SWAN + ADCIRC simulation. A random-phase JONSWAP spectrum was assumed as SWAN + ADCIRC did not pass full spectral information at all locations. The maximum period used was 25 s and the minimum period was computed dynamically from the limit of accuracy in Boussinesq dispersion.

The moving water–land interface was monitored throughout the simulation and its largest inland distance retained as the maximum wave runup inundation. Runup was found to be strongly wave group dependent (Stockdon et al., 2006), with greatest runup occurring on infragravity time scales. Runup was computed for 735 transects on Oahu and another 443 on Kauai at approximately 500 m spacing around each island. In areas with rapid changes in shoreline properties, this one-dimensionality introduces some additional uncertainty when compared to the full two-dimensional problem. The one-dimensional transects thus represent a compromise between accuracy and efficiency that will yield much improved runup results when compared to phase-averaged models, but may eventually be superseded as computational technologies improve. A further approximation in the runup computations was that a bare earth representation was used: i.e. no buildings were included in the transects. In developed areas, or in highly vegetated regions, this leads to computed runup being conservative, so results given here are an upper limit. Similar bare earth assumptions are made in tsunami inundation studies (Tang et al., 2009; Cheung et al., 2011). Again, as technologies improve this limitation may be superseded.

## 2.3. Synthetic storm parameters

Storm characteristics used in this study were developed based on guidance from the Central Pacific Hurricane Center, with tracks varying from East of Oahu to West of Kauai. Central pressures used were 970, 955, and 940 mbar, roughly corresponding to Saffir–Simpson category 2, 3, and 4 storms. A modified Rankine vortex formulation (Cheung et al., 2003) was again used to compute all wind fields. The radius of maximum winds varied from 30 km to 60 km, forward speeds varied from 7 to 22 knots (3.6–11.3 m/s), and up to five different approach angles were used for each landfall location. As might be expected, this provided a large number of

**Table 1**

Number of large scale computational runs for each landfall/track/central pressure (643 total runs).

Landfall	Track					Central Pressure (mbar)		
	A	B	C	D	E	970	955	940
0	9	6	9	8	8	13	14	13
1	9	9	9	9	9	15	15	15
2	15	16	14	18	13	23	28	25
3	5	8	5	8	8	11	10	13
4	8	8	9	9	9	15	15	13
5	14	14	14	16	16	29	20	25
6	6	7	7	7	7	15	10	9
7	12	13	13	14	14	30	9	27
8	8	9	6	7	7	11	14	12
9	13	14	14	14	14	30	10	29
10	9	9	9	9	9	15	15	15
11	12	13	14	0	1	17	6	17
12	6	5	5	0	0	4	6	6
13	6	6	0	0	0	4	4	4
14	6	6	0	0	0	4	4	4

potential storm scenarios, and not all parameter combinations were employed. Table 1 shows the number of storms used for different combinations of landfall longitude (0–14), angle of approach (A–E), and central pressure (940, 955, 970 mbar). Landfall location, angle of approach and central pressure proved to be the most important factors in determining inundation, and the radius of maximum winds and storm speed had lesser effects.

Because of these assumptions, the results shown here are close to worst-case scenarios in the event of direct landfalls. They provide an estimate of the dangerous regions, which may then be used by emergency managers or other officials as guidance for decision making. Because the Hawaiian Islands generally have a low occurrence of tropical cyclones, the probability of any given location experiencing the inundation shown here is quite low. However, as the example of Iniki shows, strong storms do impact the Hawaiian Islands and should be expected to do so in the future.

The work presented here is very closely related to, and forms the basis of, a tool for the fast prediction of inundation and wave properties for tropical cyclones in the Hawaiian Islands (Taflanidis et al., 2011). This tool, named Hakou, uses results from these pre-computed runs to create response surfaces of water level, wave heights and runup for hundreds of thousands of locations based on input tropical cyclone parameters of landfall location and angle, central pressure, forward speed, and radius of maximum winds. Incoming storms are characterized in terms of these known or predicted parameters, and the response surface is used to estimate inundation with minimal computational cost. Because of the great speed, this is also extended to ensemble estimations where thousands of scenarios may be computed to provide a statistical measure of inundation potential for a storm that is still some distance from landfall.

**Table 2**

List of all locations shown on maps.

Oahu locations		Kauai locations	
A	Kahe Power Plant	A	Kekaha
B	Kapolei Refinery	B	Waiimea
C	John Rodgers Air Field	C	Pakala
D	Ewa Beach	D	Hanapepe/Eleele/Port Allen
E	Pearl Harbor	E	Poipu
F	Hickham Air Force Base		
G	Honolulu International Airport (HNL)		
H	Low-Lying Industrial Region		
I	City Hall Downtown		
J	Waikiki		
K	Diamond Head		
L	Hawaii Kai		

### 3. Hurricane Iniki comparisons

Fig. 1 shows the track of Hurricane Iniki, and its landfall on the southern shore of Kauai. Iniki is particularly important because it is the only major hurricane with measurements for comparison in the Hawaiian Islands. In many parts of Kauai, a clear debris line was visible and was employed by Fletcher et al. (1995) and Cheung et al. (2003) to develop runup inundation maps. Here, we use these runup inundation data for several purposes: both to compare to the modeled results, and as a means of differentiating the impacts caused by the wind, wave, and surge components. Additionally, we can compare against NOAA buoy and tide measurements taken during the storm. Here Iniki was modeled using a modified

Rankine vortex model, with track, wind speed, and central pressures taken from the historical NOAA records. Because Iniki was an older storm, and was significantly asymmetric, the wind fields are not as accurate as with reconstructions in some later storms such as Hurricane Katrina, and this appears to be the greatest limit on accuracy.

#### 3.1. Wave and water level comparisons

Waves and water levels during Hurricane Iniki were measured at several stations that provided continuous information. Water level comparisons are given in Fig. 2 at Nawiliwili Harbor and Port Allen. Agreement at Nawiliwili is reasonable, with a good

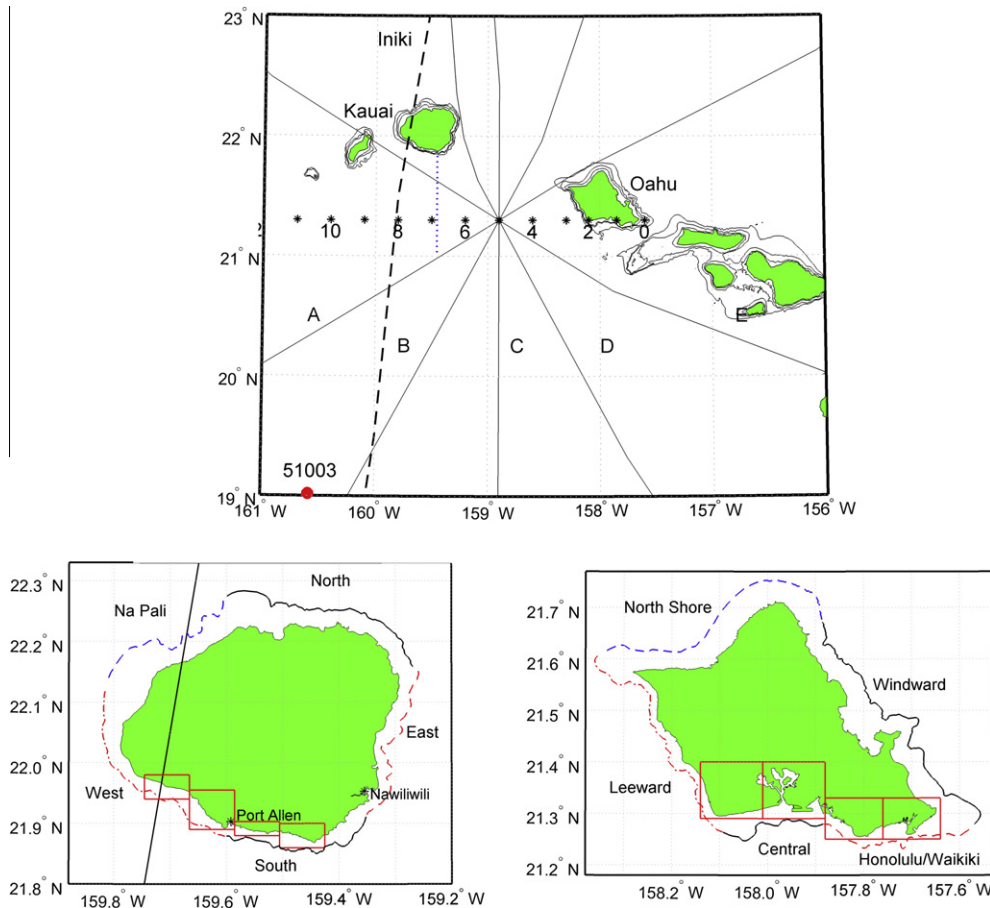


Fig. 1. Study region, showing (top) islands of Oahu and Kauai; definition of hurricane track angles A-E; landfall locations 0-14; track of Hurricane Iniki (-); location of transect for Hurricane Iniki surge (---); (•) NOAA buoy 51003. 50 m, 150 m, and 500 m bathymetric contours are shown. (Bottom) Definitions and names of different regions for Kauai and Oahu with lines at approximate 150 m depth contours; (boxes) outlines of finer scale maps.

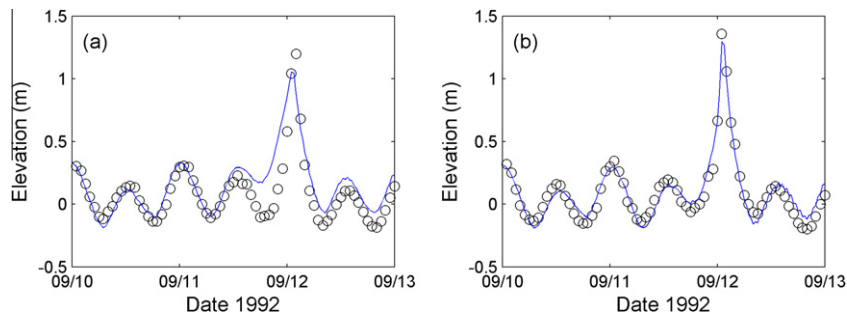
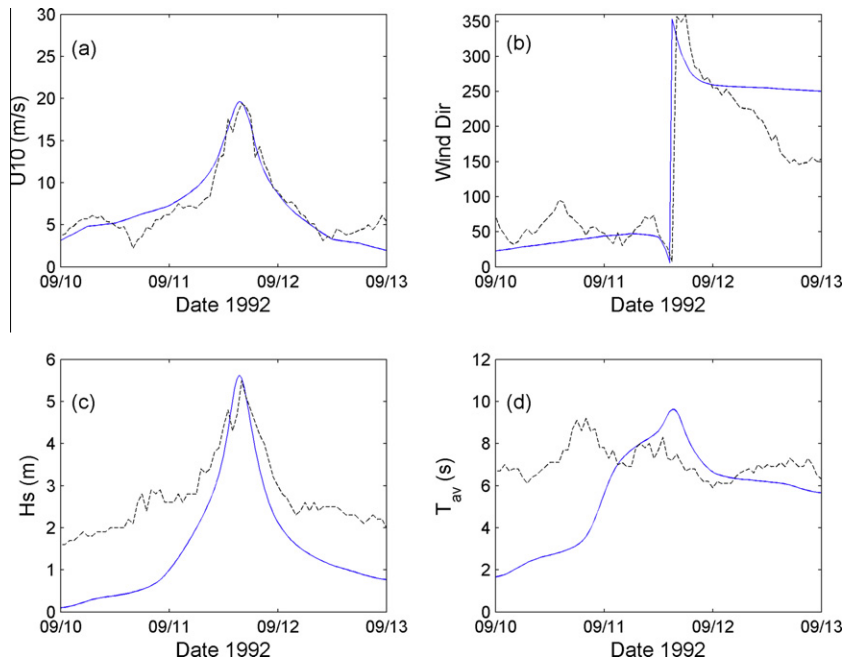


Fig. 2. Water level measurements (o) and computations (-) at (a) Nawiliwili Harbor; and (b) Port Allen during Hurricane Iniki.



**Fig. 3.** Time series of measured (–) and modeled (–) waves and winds at NDBC buoy 51003 during Hurricane Iniki. (a) 10 m wind strength; (b) wind direction; (c) significant wave height; (d) average period.

simulation of tides pre-storm, a somewhat larger early rise in computed water levels, and maximum water levels that agree to better than 15 cm. As will be seen, maximum inundation levels are many times larger than the just over 1 m surge predicted here, and are driven by runup over the steep shorelines, so this small difference in predicted and measured water levels is a minor source of error. Port Allen on the south shore of Kauai shows a similar picture, with around 1.4 m maximum measured surge, and good agreement with computed surge throughout the storm. These surge levels are very low for a Category 4 hurricane like Iniki and, as will be shown, are a result of the steep offshore bathymetry around Kauai.

Wave comparisons at deep water NOAA buoy 51003 seen in Fig. 3 have quite good agreement with peak heights, but show more error on the rising and falling limbs. Mean wave periods are too small near the beginning of the simulation and then are reasonable although with error of up to 2 s near and after the storm peak. These errors likely have two sources: (1) The finite simulation length of the hurricane before it reached 51003 did not allow for wave heights and periods to develop earlier in the simulation, and (2) Iniki has asymmetries and appears to have been embedded in a larger synoptic scale wind field which is not included in our model. This is unlike more recent storms which have much more complete wind fields available to drive waves and water levels – the same coupled SWAN + ADCIRC system has been previously used with good results in Hurricanes Katrina, Rita, and Gustav (Dietrich et al., 2011). The less complete information for Iniki leads to commensurate errors in wave heights and periods.

### 3.2. Storm inundation in Kauai

Figs. 4 and 5 show the measured and modeled inundation along the south and east coasts of Kauai, for all of the boxes shown in Fig. 1. Comparison between measured debris lines and modeled values show inundation overpredicted in some regions while underpredicted in others, but estimates are reasonable on average. In Fig. 4, Kekaha (A) and Waimea (B) are very close to landfall. Kekaha shows predicted still water inundation extending quite far inland in one location, but this is quite shallow, with almost all

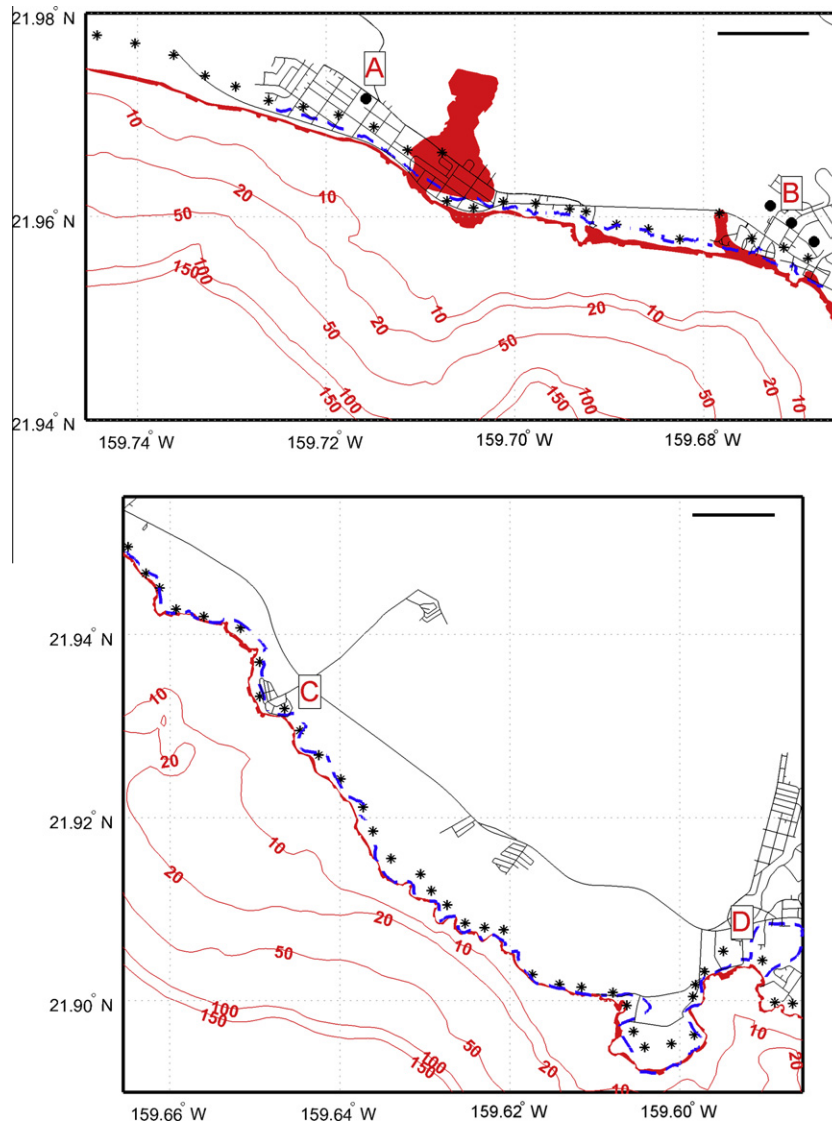
depths above ground less than 0.3 m. Wave runup shows a much greater correspondence with measured debris lines, although the agreement is not exact. A similar story is found moving farther east to Pakala Village (C) and the Port Allen area which includes Hanapepe and Elelee (D). All measured and modeled inundation is small over much of this area as the small cliffs limited penetration, although some areas do show measured and modeled penetration to several hundred meters inland.

Fig. 5 shows Iniki inundation moving further east. Both predicted and measured inundation is small along a largely uninhabited region east of Port Allen, but then increases significantly toward Poipu (E), which saw severe inundation/runup to hundreds of meters inland. Correspondence between predicted and measured inundation is quite reasonable.

In contrast to the modeled runup lines, the surge inundation modeled by SWAN + ADCIRC is much lower in many cases, and consistently underpredicts inundation levels. This is because this phase-averaged computation does not account for the intra-wave and wave group-driven runup which may intermittently add several meters to the spectrally-averaged radiation stress driven wave setup. Clearly, any inundation prediction on a steep volcanic island needs to account for wave runup. Additionally, because of the very small region of shallow water surrounding Kauai, surge levels are extremely small for a storm as strong as Iniki.

### 3.3. Iniki-in-Louisiana

Iniki's comparatively low surge level may be demonstrated by moving the track of Hurricane Iniki to Louisiana, giving it the same landfall location as Hurricane Katrina as shown in Fig. 6, and re-computing surge. Fig. 7 show results from the two computations: Iniki-in-Kauai and Iniki-in-Louisiana, along the transects shown in Figs. 1 and 6, which are the same distance from landfall. Bathymetries are in no way similar: the Kauai bathymetry in Fig. 7(a) drops off very quickly to more than 4000 m within 75 km of the shoreline. In contrast, the Louisiana transect depths are extremely shallow for 200 km south of the transect's northern end. This transect also includes some very low-lying land areas in



**Fig. 4.** Hurricane Iniki comparisons between measured and modeled inundation. Measured Debris Lines (blue dashed lines); Modeled SWAN + ADCIRC + Boussinesq Runup along transects (black stars); SWAN + ADCIRC inundation (red filled-in area); Black circles are emergency shelters. A 1 km reference line is shown in the upper portion of each subfigure.

the Mississippi Delta which are inundated during Iniki-in-Louisiana's landfall and, as seen from Eq. (1), shallow depths lead to larger surge from wind stresses. This great difference in surge is demonstrated in Fig. 7(b), where Iniki-in-Kauai shows only a 1.3 m maximum surge, almost all of which occurs at the immediate shoreline. This contrasts greatly with Iniki-in-Louisiana, which develops a classical increase in surge over the shallow bathymetry, with some complexities over the Mississippi delta and marshlands, to 4.75 m at the northern end of the transect. The difference in surge is attributable entirely to differences in depth, as both experienced identical wind conditions.

By re-running Iniki-in-Kauai without wave radiation stresses, as shown in Fig. 7(c), the impacts of waves on surge inundation are illustrated. This close-up of surge immediately offshore of the coast shows that the surges are essentially identical with and without waves until the large storm waves begin to break. For the no-wave simulation, the shoreline surge is very small – around 0.4 m, which is nearly 1 m less than with waves. This difference in still water surge may be entirely attributed to wave setup, and further underscores the differences between surge in volcanic islands, where

waves are extremely important, and continental regions where surge is dominated by wind shear stresses acting on the shallow topography (e.g. Kim et al., 2008). For planar slopes, we may even find analytical storm surge solutions from wind stress only (Dean and Darymple, 1991) to give further insight. These are entirely dependent on the dimensionless parameter  $(\tau_s/\rho gh_0)(l/h_0)$ , which is the dimensionless wind stress multiplied by the dimensionless length of the system. Iniki-in-Louisiana has both a larger dimensionless stress (because of the smaller depth  $h_0$ ) and larger dimensionless length (smaller depth and longer length of continental shelf  $l$ ) than Iniki-in-Kauai, so the great difference in wind surge is explained.

#### 4. Inundation over different regions of Oahu and Kauai

Although they can be devastating, hurricane landfalls in the Hawaiian Islands are infrequent enough that reliable return period statistics are difficult to develop. However, potential scenarios may still be developed based on historical tracks and a knowledge of

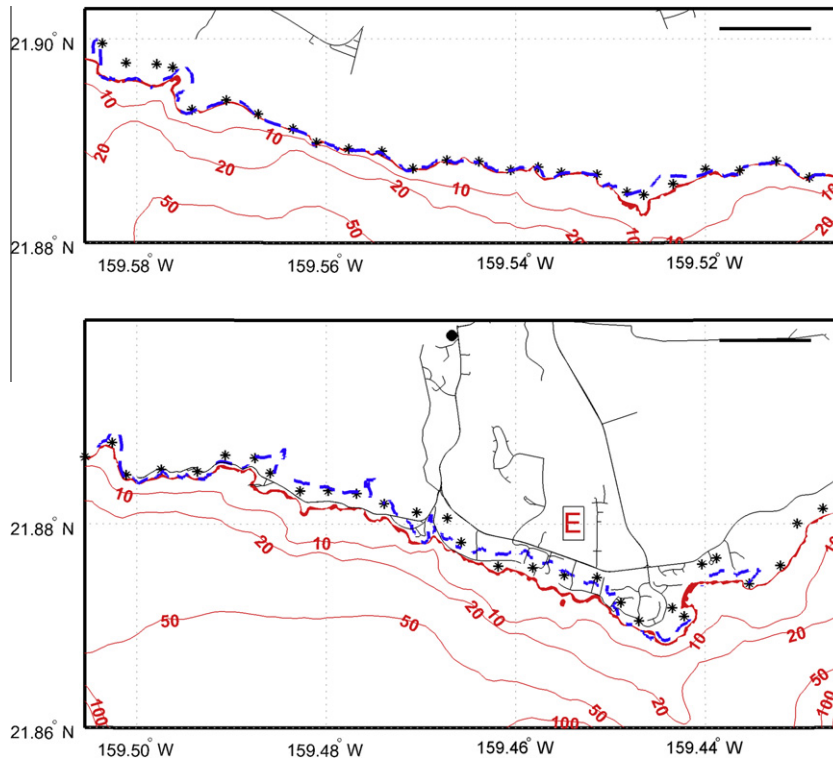


**Fig. 5.** Hurricane Iniki comparisons between measured and modeled inundation. Measured debris lines (blue dashed lines); modeled SWAN + ADCIRC + Boussinesq runup along transects (black stars); SWAN + ADCIRC inundation (red filled-in area); Black circles are emergency shelters. A 1 km reference line is shown in the upper portion of each subfigure.

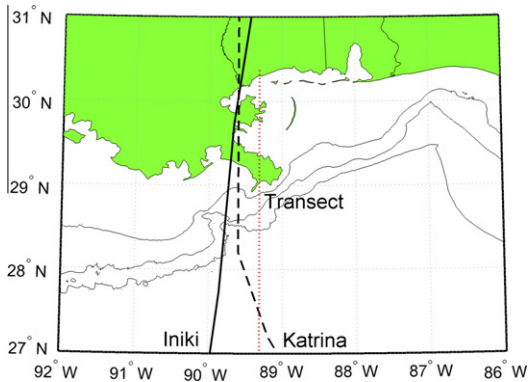


**Fig. 6.** Hurricane Iniki landfall in Louisiana at the same location as Katrina. 50 m, 150 m, and 500 m bathymetric contours are shown.

weather patterns. Using input from the Central Pacific Hurricane Center (<http://www.prh.noaa.gov/hnl/cphc/>), a suite of scenarios was developed and SWAN + ADCIRC and Bouss1D model runs were performed for 643 storms in the vicinity of Oahu and Kauai. Fig. 1 shows the nominal landfall locations 0–14, which were simply different longitudes that each storm would pass through at 21.3°N, and the five tracks A–E, which had different headings at the landfall location. Table 1 shows combinations of landfall location/track angle and landfall location/central pressure, to give an idea of the parameter combinations employed here. Radius of maximum winds and forward speed were the two other parameters used here: these also affected results, but proved somewhat secondary in importance when compared to geographic location parameters and central pressure.

With this large number of scenarios, it becomes necessary to aggregate information, and the most fundamental aggregate

quantity is the maximum inundation experienced during any storm. Thus, the results presented in this section represent the maximum water levels and runup for any of the storms, and give the near-worst case scenarios for inundation. Of course, this so-called max of max inundation does not provide information on how waves and water levels varied under other conditions: these will be explored in a later section.

#### 4.1. Oahu

With more than 950,000 residents, the Island of Oahu is the most densely populated location in the Hawaiian Islands, with twice the number of people of all of the other Islands combined (US Census Bureau, <http://www.census.gov/>). This number is augmented by the more than four million annual visitors to Oahu (Hawaii Visitor and Conventions Bureau, <http://www.hvcb.org/>), most of whom are based on the south (more exposed to hurricanes) side of the island in Honolulu and Waikiki. When coupled with the knowledge that much of the most densely populated and most visited regions are only marginally above sea level, a major hurricane landfall on Oahu would have larger repercussions than on any of the other Islands.

##### 4.1.1. Southwest Shore of Oahu: Barber's Point and Kahe Power Plant, Pearl Harbor and Honolulu Airport to Sand Island

Fig. 8 shows maximum inundation for all simulated storms on the south portion of the Leeward shore of Oahu, and the western portion of Central Oahu. Located at the northern portion of the figure, Kahe Power Plant (A) supplies Honolulu with electricity and is thus an essential service. Surge predictions in this region are confined to the ocean side of the Farrington Highway. However, runup computations show waves potentially crossing the road to the power plant property. These are confined to the most seaward portion of the property where elevations are lower, but there could

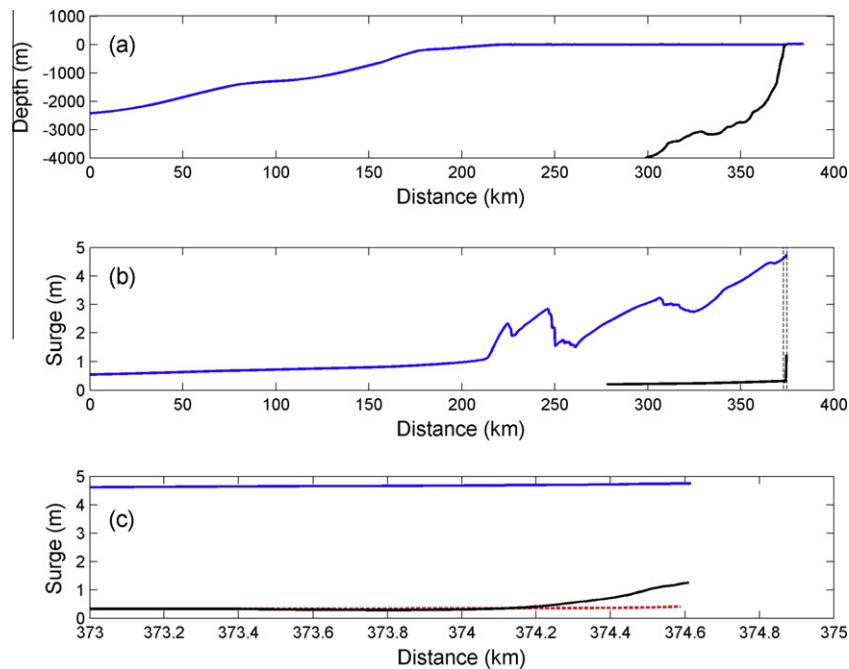


**Fig. 7.** Comparisons between Hurricane Iniki landfalls in Kauai (black) and in Louisiana (blue) over transects shown in Figs. 1 and 6. (a) Depth; (b) surge along transect; (c) near-coast detail of surge between vertical dashed lines in (b). The red dashed line shows Iniki surge in Kauai computed without wave radiation stresses.

be small waves near the power plant facilities. South of Barbers Point Harbor, on the far southern portion of the Leeward Shore, both surge and runup show penetration of the Kapolei Refinery (B) over regions that include plant machinery. This is an extremely low-lying area and could experience significant flooding in the event of a direct landfall. Potential inundation continues to be significant in the region of John Rodgers Air Field (C), with both waves and surge nearing the US Coast Guard Air Station Barbers Point and further east to 158.025°W. Fortunately, these areas are lightly inhabited.

From Ewa Beach (D) east to Pearl Harbor, the coastline becomes much more developed and the topography continues to be low. Inundation may reach up to half a kilometer or more inland, covering several streets. These are clearly danger areas in the event of a direct landfall. In contrast, inundation has relatively moderate potential in the inner Pearl Harbor region (E), as waves even during storms are quite small and thus cannot generate large runup. Some areas near the north end of the harbor have low lying ground, and thus can see significant surge inundation in the worst case scenarios. Near the East Entrance to Pearl Harbor, inundation potential increases strongly, with submerged regions at Hickham Air Force Base (F) reaching more than 1 km inland in these low-lying areas. Areas of potential wave action also progress hundreds of meters inland, although once again these neglect the influence of buildings. The Honolulu International Airport (G) is also quite low-lying and is certain to experience significant inundation to hundreds of meters inland in the event of a direct impact from a strong storm. Similar inundation is predicted to occur northeast of the airport in the low-lying industrial region between Interstates H1 and H201 (H).

In addition to hurricanes, the Hawaiian Islands are subject to tsunamis, which have caused considerable damage at some locations (Tang et al., 2009). Thus, the State of Hawaii has declared certain areas to be tsunami evacuation zones, which are activated in the event of a tsunami-generating earthquake elsewhere in the Pacific. There are clear similarities between tsunami inundation and hurricane wave runup inundation, as both are transient processes with alternating advance and retreat cycles that may increase penetration significantly over the local still water level. However,

tsunamis have much longer periods and do not form on top of a locally elevated surge, as is the case with hurricane runup. Direct comparisons between tsunami zones and the present inundated areas show rough equivalence with wave runup inundation in some areas, particularly on exposed coasts near the Kapolei refinery (B) and John Rodgers Air Field (C). However, in low-lying regions where still water surge dominates such as inner Pearl Harbor (E) or Hickham Air Force Base (F), there is less correlation. Thus, the tsunami evacuation zones should not blindly be used as a proxy for hurricane inundation.

#### 4.1.2. Southeast shore of Oahu: Downtown Honolulu, Waikiki, Hawaii Kai to Makapuu Point

The portion of Honolulu east of the airport (G) through to Waikiki (J) and west of Diamond Head (K) is the most populated part of Oahu, and also has considerable inundation potential in the event of a direct landfall. The developed coastline of Oahu between 157.88°W and 157.82°W shown in Fig. 9 is extremely low-lying and has inundation potential of well over 1 km inland. This includes not only the strongest storms, but also the weaker 955 and 970 mbar landfalls (not shown). The outer fringes of this region include several emergency shelters. Parts of downtown Honolulu near 157.86°W and near City Hall (I) are at slightly higher elevation and are predicted to remain dry during all computed storms.

Inundation potential becomes much worse east of downtown, through Waikiki and to Diamond Head. Most of this region is very low-lying and was reclaimed from drained marshlands and built up to small positive elevations (Lum and Cox, 1991). Potential inundation is over 1 km inland throughout this region. The Waikiki (J) region of Honolulu, which has a very high concentration of tourists and large hotels, could experience flooding up to several kilometers inland for the strongest storms. This flooding would come not only from the ocean side, but through the Ala Wai Canal, which was created in 1928 to drain the low-lying areas that are now Waikiki. Wave runup computed with a bare earth assumption is predicted to penetrate significantly inland over much of this area, but would be limited by the large, strong buildings in this

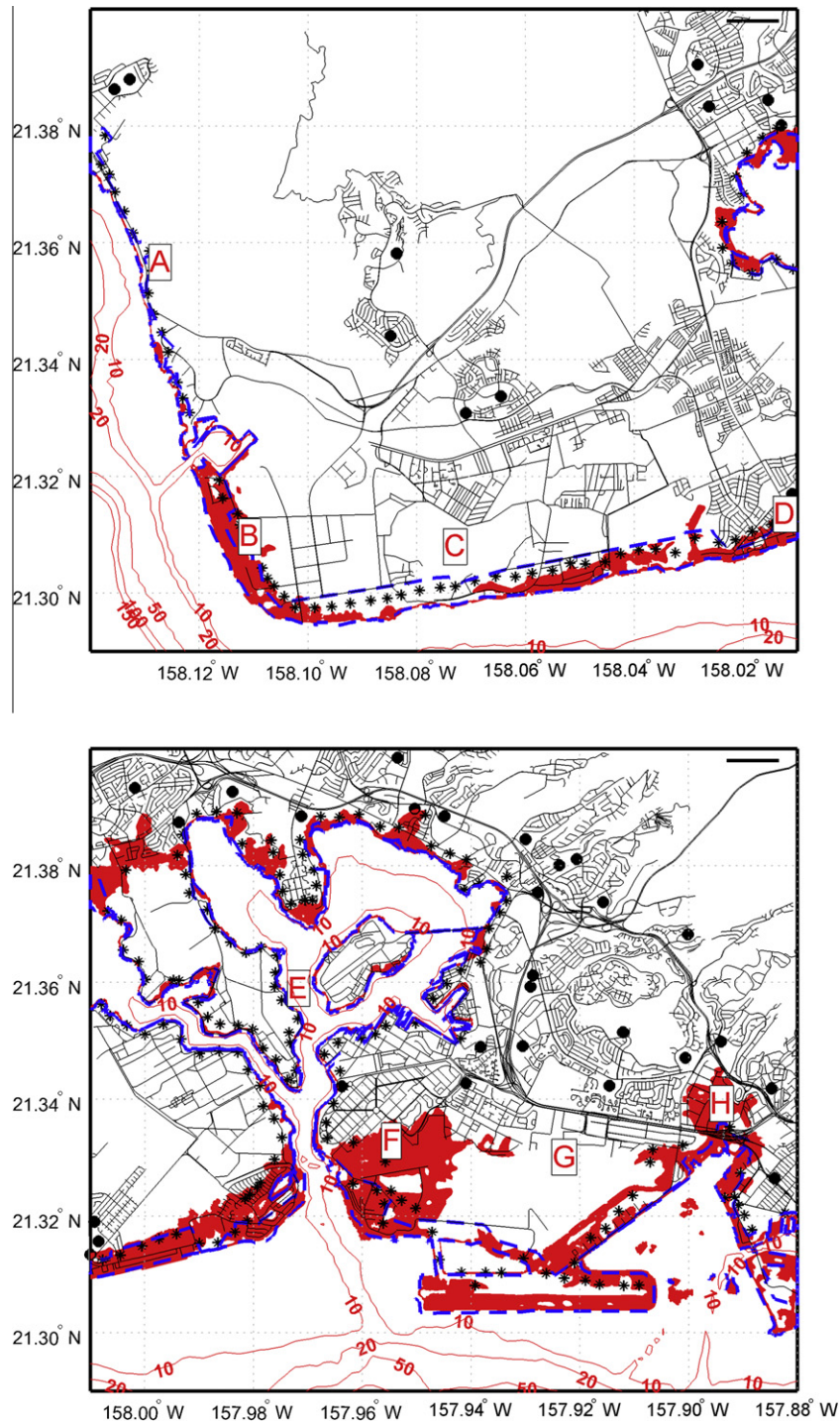


**Fig. 8.** Maximum predicted inundation extent for all computed storms, Southwest Shore of Oahu and Barbers Point east to Pearl Harbor and past Honolulu Airport. (Red regions) still water surge; (stars) wave runup; (blue dashed lines) extent of tsunami evacuation zones. Black circles are emergency shelters. Boxed letters refer to locations in Table 2. A 1 km reference line is shown at the top of each subfigure.

highly developed region. However, even in this worst case scenario, it must be noted that the flooding depths would be relatively small, and would only exceed 1 m at locations quite close to the shore. Tsunami inundation zones in this region are also large, but are less than still water surge inundation limits.

Further to the east, the steep slopes of the Diamond Head (K) crater southeast of Waikiki limit inundation strongly to the immediate shoreline, but potential inundation east to Hawaii Kai (L) is significant, up to several hundred meters inland from both still

water inundation and wave runup. In this region, runup and tsunami evacuation zones are quite similar with the exception of Makapuu Point at the far eastern edge of Oahu, where tsunami zones extend much further inland.

#### 4.2. Kauai

Kauai is a much different island from Oahu, with higher elevations tending to be closer to shore, a less complex coastline, and a

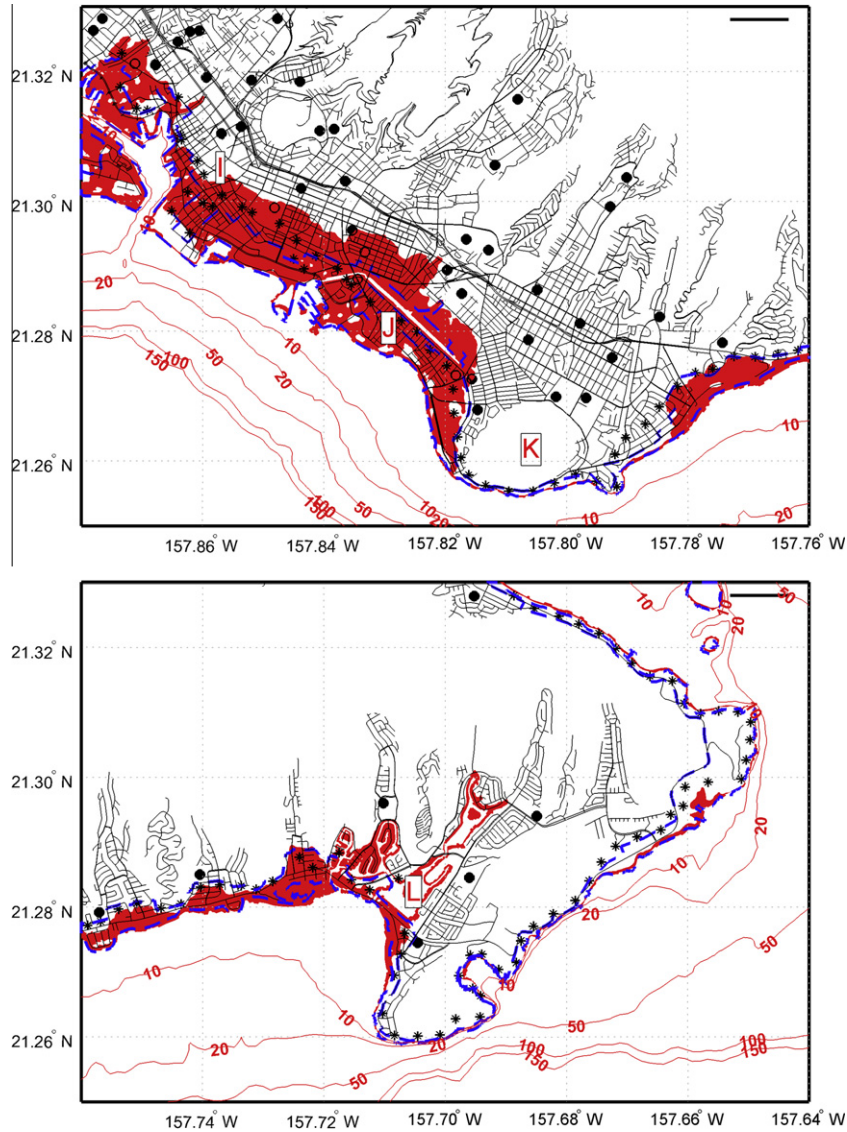


**Fig. 9.** Maximum predicted inundation extent for all computed storms, downtown Honolulu, Waikiki and Diamond Head east to Makapuu Point. (Red regions) still water surge; (stars) wave runup; (blue dashed lines) extent of tsunami evacuation zones. Black circles are emergency shelters. Boxed letters refer to locations in Table 2. A 1 km reference line is shown at the top of each subfigure.

much lower population. These act to reduce the potential for widespread inundation in populated areas. Nevertheless, as was shown by Hurricane Iniki in 1992, a direct hit from a strong hurricane will have severe consequences. Figs. 10 and 11 show maximum computed still water surge and wave runup inundation for the same regions as were shown for Iniki. This is useful, as it provides a direct comparison between computed inundation in Iniki, the storm of record in Figs. 4 and 5, and the maximum inundation computed by the present scenarios. Two items become apparent from this. The first is that Iniki, although very bad, was not necessarily the worst case scenario for all regions of Kauai. The second is that wave runup for Kauai is predicted to be significantly more important in most cases compared to surge.

4.2.1. Kekaha and Waimea east to Hanapepe/Eleele/Port Allen

Fig. 10 shows significant still water surge predicted around Kekaha (A) and into Waimea (B) although, again, flooding depths above ground level are not predicted to be large. Wave runup is predicted to penetrate well into the towns, and considerably farther than observed Iniki debris lines in Fig. 4. It should again

be emphasized that the wave runup lines represent the largest inland penetration by any wave, which would have been quite small by the time it reached this region, and that a bare earth assumption was used for all computations, which will make runup estimates conservative. Tsunami evacuation zones here appear to be similar to wave runup maxima over much of these towns.

Farther southeast towards Pakala (C) and Hanapepe/Eleele/Port Allen (D), still water inundation does not ever leave the immediate coastal slope, making it a negligible concern, while predicted wave runup may penetrate several hundred meters inland for the strongest storms. Both hurricane inundation distances are considerably less than the extent for the tsunami inundation zone, which extends nearly 1 km inland in some places.

4.2.2. East of Port Allen to Poipu

Continuing southeast, Fig. 11 shows a lightly inhabited, largely agricultural, section of coastline between 159.58°W and 159.51°W, with cliffs exceeding 10 m in height. There is no significant inundation predicted along this stretch of coastline for any storm, and the tsunami zones show a similar small extent. Further east towards

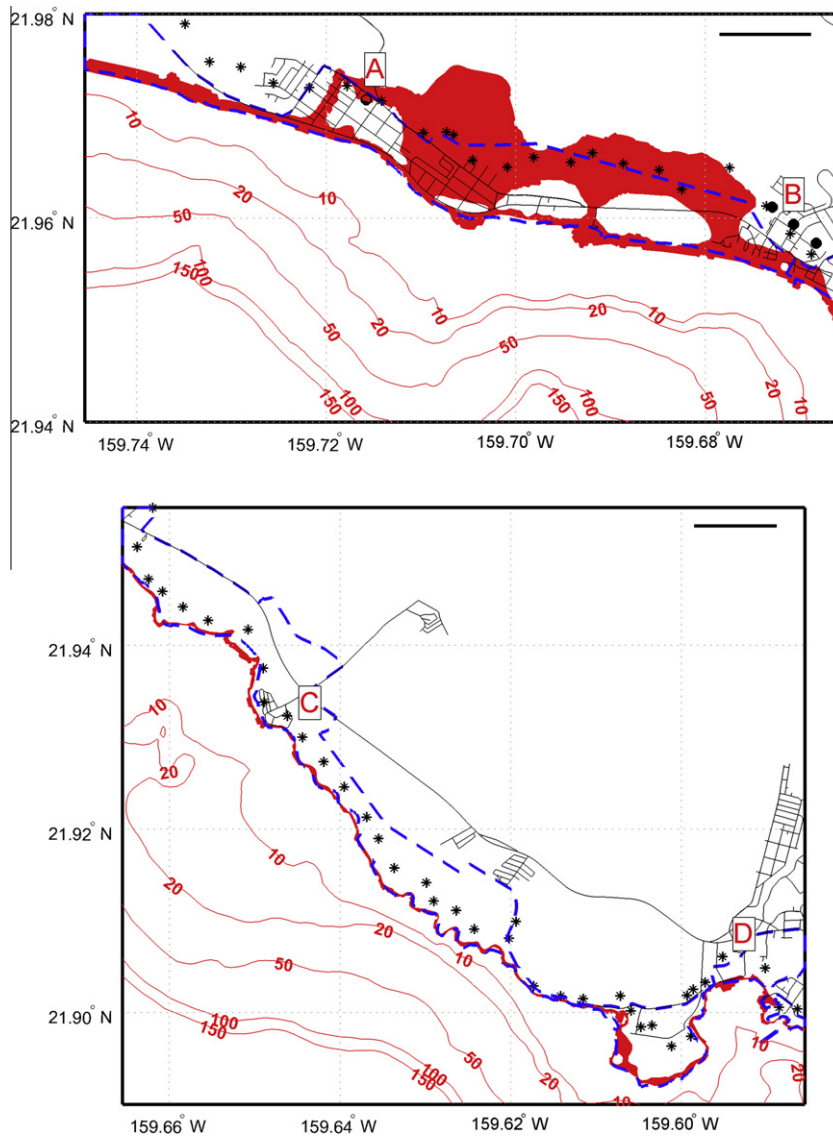


**Fig. 10.** Maximum predicted inundation extent for Kauai for all computed storms. (Red regions) still water surge; (stars) wave runup; (blue dashed lines) extent of tsunami evacuation zones. Black circles are emergency shelters. Boxed letters refer to locations in Table 2. A 1 km reference line is shown at the top of each subfigure.

Poipu (E), these cliffs reduce in size to where runup is predicted to exceed their height and penetrate over the much flatter built-up landscape. However, still water surge is still predicted to remain largely below the cliff-tops. These predictions are in accordance with observations during Iniki, where the runup line did penetrate significantly inland in this region. Here, wave runup is predicted to exceed the tsunami evacuation zone by hundreds of meters.

### 5. Wave height and water level envelopes

Because it is often useful to have an overall estimate of inundation for a given storm strength and general location, islands were divided into regions as defined in Fig. 1 (taken from <http://www.hawaii-guide.com/>), still water surge and significant wave heights in these regions were extracted for all storms, and results were separated according to storm characteristics (central pressure and landfall location). Next, for each storm in the database, all wet nodes on what is normally dry land were sorted by elevation, and the 99th percentile of surge was computed for each storm. Using the 99th percentile instead of the maximum surge eliminated a

few poorly resolved points which had very large anomalous surge elevations over one or two elements. Again, all simulations were run at a high tide of 0.4 m, so this becomes the lowest possible water level. For each storm, once the 99% surge was computed for each storm in each subregion, results were sorted by central pressure, and also by nominal landfall location 0–14. These gave a rough indicator of the storm strength and location to see how surge quantities varied with changing storm characteristics. For each combination of landfall location and central pressure, the maximum 99% surge for any storm, minimum 99% surge found during any storm and average of the 99% surge for all storms were found for each island subregion, and plotted in Figs. 12 and 13.

#### 5.1. Overland 99% surge values

For 99% surge values, it is first noteworthy that nowhere do they exceed 3 m elevation and only a few storms have greater than 2.5 m elevation, both including the 0.4 m high tide elevation as part of the surge. This is much lower than can be found in areas with a wide continental shelf, as shown by the example of Iniki-in-Louisiana in Fig. 7. There is a clear correlation between low

central pressures and high surge, although the envelope can vary by over 1 m for storms with the same nominal landfall location and central pressure. With the exception of the sheltered Kauai Na Pali Coast, which has a maximum 99% surge elevation of

1.8 m, all regions of both Oahu and Kauai see a maximum 99th percentile surge of between 2.5 m and 2.9 m. Unsurprisingly, maximum surge levels occur when tracks are such that strong winds blow directly towards these coasts: low number landfall

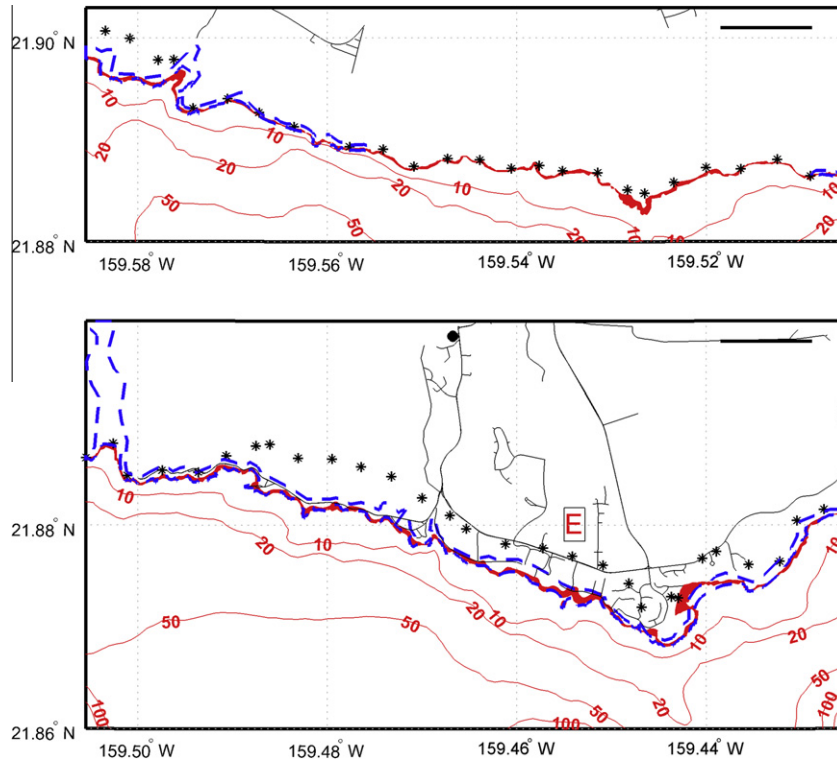


**Fig. 11.** Maximum predicted inundation extent for Kauai for all computed storms. (Red regions) still water surge; (stars) wave runup; (blue dashed lines) extent of tsunami evacuation zones. Black circles are emergency shelters. Boxed letters refer to locations in Table 2. A 1 km reference line is shown at the top of each subfigure.

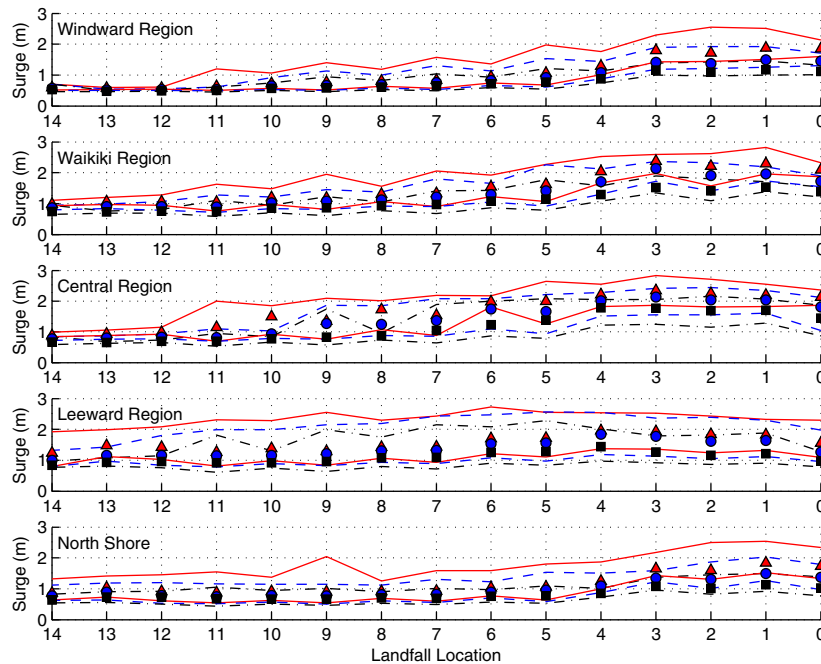


**Fig. 12.** Storm surge (99%) max, min, and average for all regions of Oahu shown in Fig. 1. Solid red lines are 940 mbar results, dashed blue lines are 955 mbar; dash-dot black is 970 mbar. The top line for each central pressure is the highest 99% surge for any storm; the lowest line is the smallest 99% surge; symbols are average of 99% surges for 940 mbar (triangles), 955 mbar (circles), and 970 mbar (squares).

locations (which are further east) tend to produce higher surge for the Windward Coast of Oahu and, similarly, high landfall locations (which are further west) produce large surge for the Kauai West region.

5.2. 99% Significant wave heights

Statistics of runup elevation are not shown, as these were dominated by waves impacting on high cliffs where maximum runup

elevations could be very large but the distance inland very small. Still, because waves are so important we have provided wave height statistics at the 150 m bathymetric contour, where waves propagating from the deep ocean have not yet begun to be influenced by the island. For the Hawaiian Islands, the 150 m depth contour is very close to shore, usually within a few kilometers as seen in Fig. 1, so these are the conditions that will directly affect the shoreline and runup. Wave heights were sorted by region as with the surge, ordered so that the 99th percentile could be found,

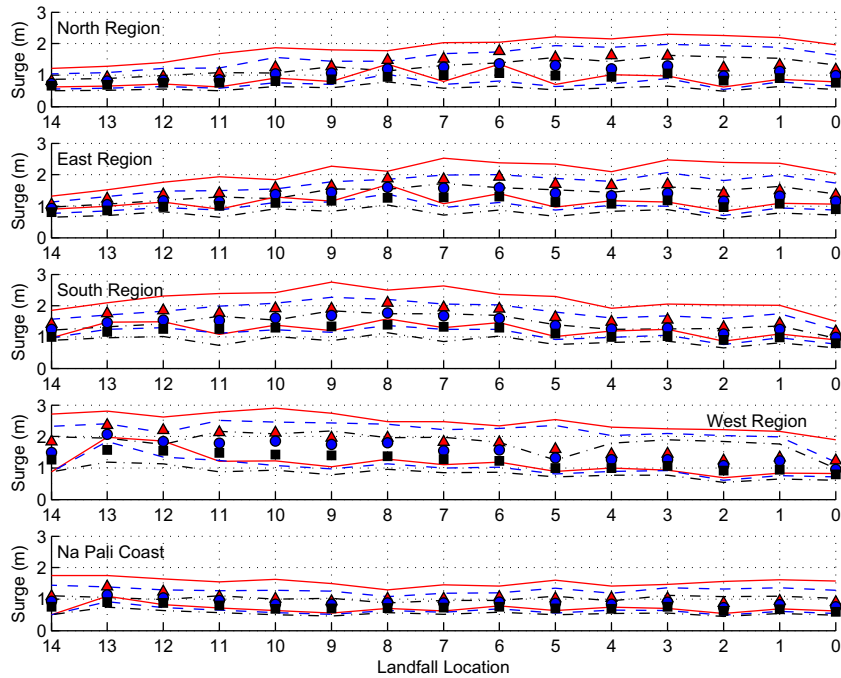


Fig. 13. Storm surge (99%) max, min, and average for all regions of Kauai shown in Fig. 1. Lines and symbols are identical to Fig. 12.

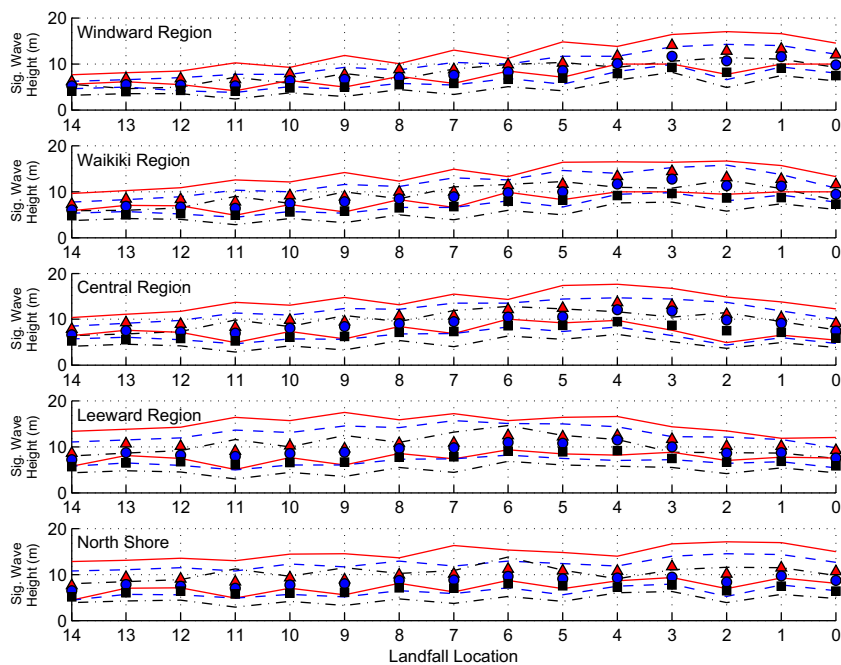


Fig. 14. Significant wave heights at 150 m contours of Fig. 1: (99%) max, min, and average for all regions of Oahu at 150 m depth contours of Fig. 1. Lines and symbols are identical to Fig. 12.

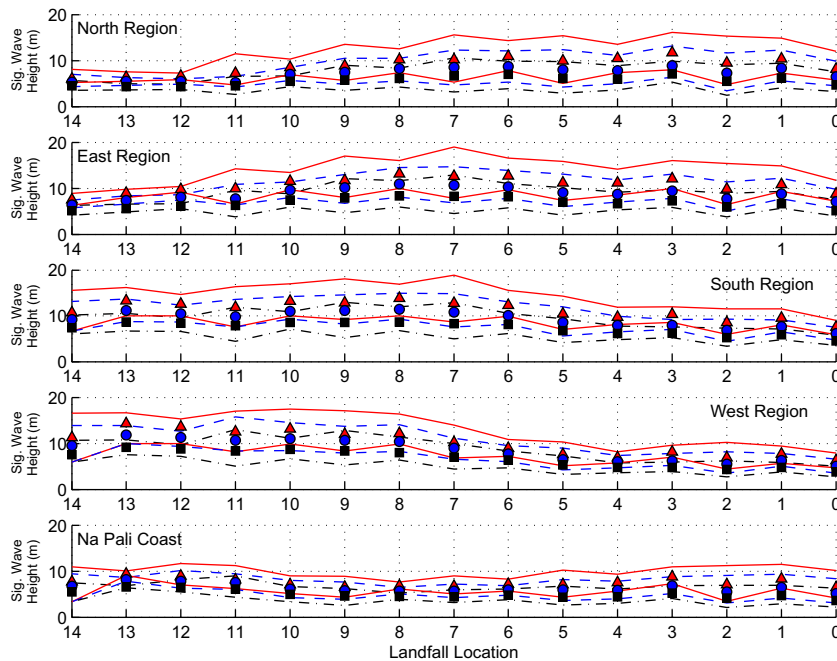


Fig. 15. Significant wave heights: (99%) max, min, and average for all regions of Kauai at 150 m depth contours of Fig. 1. Lines and symbols are identical to Fig. 12.

and plotted in Figs. 14 and 15. Unsurprisingly, wave heights are largest for coasts with direct exposure to the storm track, and for stronger storms. The range of maximum significant wave heights also varies, but can exceed 10 m for a variety of storms. For the most extreme cases, 99th percentile significant wave heights exceed 18 m on the South and East shores of Kauai, and on most of Oahu. The North Shore of Oahu and the Na Pali Coast of Kauai show the smallest heights as they are to some degree sheltered from the southerly and easterly hurricane waves. This is notable as the Oahu North Shore is known for the large winter waves that establish its status as a surfing destination (Caldwell, 2005).

In addition to the maxima of the wave height envelopes, the minima are also of interest. For both Oahu and Kauai, for storms with central pressures varying between 940 mbar and 970 mbar, it is difficult (although possible) to find storms with significant wave heights less than 4 m on any coast of either island. This shows that no matter what the details of the storm tracks and strengths, the large open ocean fetches and deep water combine to give large wave heights around all islands, and will create conditions that are still dangerous far from landfall.

## 6. Conclusions

The lack of a continental shelf and relatively steep slopes of the Hawaiian Islands are a double-edged sword for storm inundation. Still water surge levels for a given storm will be greatly reduced over mainland locations, and for our computations do not exceed 3 m in either Oahu or Kauai for any of the 643 synthetic storm scenarios tested. The example of Iniki making landfall in Kauai compared to if it had made landfall in southern Louisiana demonstrates the large reduction in surge from 4.8 m in Louisiana to 1.3 m in Kauai as a direct result of the deeper, steep-sloped bathymetry. However, the lack of a continental shelf means that nearshore wave heights can be much larger and wave runup may be significantly increased along a narrow coastal strip. Significant wave heights of greater than 10 m are possible within a few kilo-

meters of shore, which is in accordance with visual observations during Hurricane Iniki (US Department of Commerce, 1993).

Although hurricane landfalls are relatively rare in the Hawaiian Islands, the example of Iniki shows that a direct hit could be catastrophic. This would also be the case for a hurricane landfall in Honolulu, which has the potential to flood much of the city, and in particular the heavily visited region of Waikiki to well over 1 km inland. Scenarios for Kauai show somewhat more limited inundation potential, although maximum inundation can be somewhat more than was seen during Iniki. Fortunately, although hurricane return periods are not known as well for the Hawaiian Islands as for some other locations, the results presented here are certainly much more conservative than the 1 in 100 year standards used for design in mainland locations. The bare earth assumption used in runup computations is also a source of conservatism in built up and densely vegetated areas, where the additional wave dissipation will reduce runup over the results presented here.

When potential hurricane inundation is compared to tsunami evacuation zones, there is a rough correspondence in many locations, but details are different – enough that tsunami zones should not simply be used as a proxy for hurricane inundation.

## Acknowledgements

This work was funded under the Surge and Wave Island Modeling Studies under the Field Data Collection Program of the US Army Corps of Engineers. Permission to publish was granted by the Chief of Engineers.

## References

- Blake, E.S., Landsea, C.W., 2011. The deadliest, costliest, and most intense United States tropical cyclones from 1851 to 2010 (and other frequently requested hurricane facts). NOAA Technical Memorandum NWS NHC-6, 47 pp.
- Bunya, S., Dietrich, J.C., Westerink, J.J., Ebersole, B.A., Smith, J.M., Atkinson, J.H., Jensen, R., Resio, D.T., Luettich, R.A., Dawson, C., Cardone, V.J., Cox, A.T., Powell, M.D., Westerink, H.J., Roberts, H.J., 2010. A high-resolution coupled riverine flow, tide, wind, wind wave, and storm surge model for southern Louisiana and

- Mississippi. Part I: Model development and validation. *Month. Weather Rev.* 138, 345–377.
- Caldwell, P.C., 2005. Validity of north shore, Oahu, Hawaiian Islands surf observations. *J. Coastal Res.* 21, 1127–1138.
- Cavaleri, L., Malanotte-Rizzoli, P., 1981. Wind wave prediction in shallow water: theory and applications. *J. Geophys. Res.* C11, 10961–10973.
- Cheung, K.F., Phadke, A.C., Wei, Y., Rojas, R., Douyere, Y.J.-M., Martino, C.D., Houston, S.H., Liu, P.L.-F., Lynett, P.J., Dodd, N., Liao, S., Nakazaki, E., 2003. Modeling of storm-induced coastal flooding for emergency management. *Ocean Eng.* 20, 1353–1386.
- Cheung, K.F., Wei, Y., Yamazaki, Y., Yim, S.C.S., 2011. Modeling of 500-year tsunamis for probabilistic design of coastal infrastructure in the Pacific Northwest. *Coast. Eng.* 58, 970–985.
- Dean, R.G., Darymple, R.A., 1991. *Water Wave Mechanics for Engineers and Scientists*. World Scientific, Singapore.
- Dietrich, J.C., Bunya, S., Westerink, J.J., Ebersole, B.A., Smith, J.M., Atkinson, J.H., Jensen, R., Resio, D.T., Luettich, R.A., Dawson, C., Cardone, V.J., Cox, A.T., Powell, M.D., Westerink, H.J., Roberts, H.J., 2010. A high-resolution coupled riverine flow, tide, wind, wind wave, and storm surge model for southern Louisiana and Mississippi. Part II: Synoptic description and analysis of Hurricanes Katrina and Rita. *Month. Weather Rev.* 138, 378–404.
- Dietrich, J.C., Zijlema, M., Westerink, J.J., Holthuijsen, L.H., Dawson, C., Luettich, R.A., Jensen, R.E., Smith, J.M., Stelling, G.S., Stone, G.W., 2011. Modeling hurricane waves and storm surge using integrally-coupled, scalable computations. *Coast. Eng.* 58, 45–65.
- Demirbilek, Z., Nwogu, O.G., Ward, D.L., Sánchez, A., 2009. Wave transformation over reefs: evaluation of one-dimensional numerical models. Coastal and Hydraulics Laboratory Technical Report ERDC/CHL TR-09-1. US Army Engineer Research and Development Center.
- Fletcher, C.H., Richmond, B.M., Barnes, G.M., Schroeder, T.A., 1995. Marine flooding on the coast of Kaua'i during Hurricane Iniki: hindcasting inundation components and delineating washover. *J. Coastal Res.* 11, 188–204.
- Kim, K.O., Yamashita, T., Choi, B.Y., 2008. Coupled process-based cyclone surge simulation for the Bay of Bengal. *Ocean Model.* 25, 132–143.
- Kennedy, A.B., Chen, Q., Kirby, J.T., Dalrymple, R.A., 2000. Boussinesq modeling of wave transformation, breaking and runup. I: 1D. *J. Waterway, Port, Coastal and Ocean Eng.* 126, 39–47.
- Lum, W., Cox, R., 1991. The Ala Wai Canal from wetlands to world-famous Waikiki. In: Ritter, W.F. (Ed.), *Proceedings of the National Conference Irrigation and Drainage Engineering*, Honolulu, pp. 474–480.
- Mase, H., 1989. Random wave runup height on gentle slope. *J. Waterway, Port, Coastal Ocean Eng.* – ASCE 115, 649–661.
- Mastenbroek, C., Burgers, G., Janssen, P.A.E.M., 1993. The dynamical coupling of a wave model and a storm surge model through the atmospheric boundary layer. *J. Phys. Oceanogr.* 23, 1856–1866.
- Nwogu, O., 1993. Alternative form of Boussinesq equations for nearshore wave propagation. *J. Waterway, Port, Coastal Ocean Eng.* – ASCE 119, 618–638.
- Nwogu, O., Demirbilek, Z., 2010. Infragravity wave motions and runup over shallow fringing reefs. *J. Waterway, Port, Coastal Ocean Eng.* – ASCE, 295–305. [http://dx.doi.org/10.1061/\(ASCE\)WW.1943-5460.0000050](http://dx.doi.org/10.1061/(ASCE)WW.1943-5460.0000050).
- Post, Buckley, Schuh, & Jernigan, Inc., 1993. Hurricane Iniki Assessment.
- Stockdon, H.F., Holman, R.A., Howd, P.A., Sallenger, A.H., 2006. Empirical parameterization of setup, swash, and runup. *Coast. Eng.* 53, 573–588.
- Taflanidis, A.A., Kennedy, A.B., Westerink, J.J., Smith, J., Cheung, K.-F., Hope, M., Tanaka, S., 2011. Probabilistic hurricane surge risk estimation through high fidelity numerical simulation and response surface approximations. In: Ayyub, B.M. (Ed.), *Proceedings of the International Conference on Vulnerability and Risk Analysis and Management/Fifth International Symposium on Uncertainty Modeling and Analysis (ISUMA 2011)*, Hyattsville. [http://dx.doi.org/10.1061/41170\(400\)74](http://dx.doi.org/10.1061/41170(400)74).
- Tang, L., Titov, V.V., Chamberlin, C.D., 2009. Development, testing, and applications of site-specific tsunami inundation models for real-time forecasting. *J. Geophys. Res.* – Oceans 114, C12025. <http://dx.doi.org/10.1029/2009JC005476>.
- US Department of Commerce, 1993. Natural disaster survey report. Hurricane Iniki, September 6–13, 1992. 111 pp.
- Zijlema, M., 2010. Computation of wind-wave spectra in coastal waters with SWAN on unstructured grids. *Coast. Eng.* 57, 267–277.